Supporting Information

Ni/Co bimetallic organic framework nanosheet assemblies for high-performance electrochemical energy storages

Yao Chi [a], Wenping Yang [a], Yichen Xing [a], Yan Li [a], Huan Pang[a], and Qiang Xu *[b]*

[a]School of Chemistry and Chemical Engineering, Yangzhou University, Yangzhou, 225009, Jiangsu, P. R. China.

[b]AIST-Kyoto University Chemical Energy Materials Open Innovation Laboratory (ChEM-OIL), National Institute of Advanced Industrial Science and Technology (AIST), Yoshida, Sakyo-ku, Kyoto 606-8501, Japan.

E-mail: huanpangchem@hotmail.com; panghuan@yzu.edu.cn; q.xu@aist.go.jp; qxuchem@yzu.edu.cn.

1. Experiment

1.1 Materials and reagents

The reagents used for the synthesis of the Ni-MOF, $Ni(NO_3)_2 \cdot 6H_2O$, $Co(NO_3)_2 \cdot 6H_2O$, terephthalic acid, polyvinylpyrrolidone (PVP) were purchased from Aladdin. All the chemicals in this study were used as received without further purification, including nickel nitrate hexahydrate ($Ni(NO_3)_2 \cdot 6H_2O$, 99%, Beijing Chemical Works, Beijing, China), terephthalic acid (TPA, 99%+, Adamas Reagent Co., Ltd., Shanghai, China), N,N-dimethylformamide (DMF, Tianjin fuchen chemical reagents factory, Tianjin, China), ethanol (BeiJing chemical Works, Beijing, China), Nickel foam (Tianyu Science and Technology Development Co., Ltd., Heze, China). All aqueous solutions were freshly prepared with high purity water (18 MΩ cm^{-1})

1.2 Synthesis of monometallic counterparts Ni- and Co-MOF and NiCo bimetallic MOF

The Ni-MOF/Co-MOF was synthesized according to a common method: 0.15 g terephthalic acid (TPA), 1.5 g PVP and 0.2 g $Ni(NO_3)_2 \cdot 6H_2O$ or $Co(NO_3)_2 \cdot 6H_2O$ dissolved in mixture solution with the volume ratio of water: ethanol: DMF =1:1:1 at room temperature under supersonic vibration for 40 min. The mixture solution was then transferred into a 50 mL Teflon-line autoclave and kept at 150 ℃ for 600 min. After the reaction was completed, a green/red solution was obtained. This product was precipitated by adding ethanol and acetone followed by centrifugation at 12000 rpm for 5 min. Then the product was separated by centrifugation and washed 3 times with methanol, water, DMF respectively. At last the product were washed with ethanol for three times and dried in vacuum at 70 ℃ overnight. This sample is denoted as Ni-MOF/Co-MOF.

The NiCo-MOF was synthesized according to a hydrothermal method: 0.15 g terephthalic acid (TPA), 1.5 g PVP, $Ni(NO_3)_2 \cdot 6H_2O$ and $Co(NO_3)_2 \cdot 6H_2O$ with different mass ratios dissolved in mixture solution with the volume ratio of water: ethanol: DMF =1:1:1 at room

temperature under supersonic vibration for 40 min. The mixture solution was then transferred into a 50 mL Teflon-line autoclave and kept at 150 ℃ for 600 min. After the reaction was completed, the solution of varying shades was obtained. This product was precipitated by adding ethanol and acetone followed by centrifugation at 12000 rpm for 5 min. Then the product was separated by centrifugation and washed 3 times with methanol, water, DMF respectively. At last the product were washed with ethanol for three times and dried in vacuum at 70 ℃ overnight. This sample is denoted as Ni-MOF/Co-MOF.

1.3 Characterization

The morphological features were characterized by scanning electron microscopy (SEM, Zeiss-Supra 55), high resolution transmission electron microscopy (HRTEM, Tecnai G2 F30 S-TWIN) and energy dispersive spectroscopy (EDS) mapping. X-ray diffraction (XRD) patterns were examined on a Bruker D8 Advanced X-ray diffractometer (CuK_α radiation: λ = 0.15406 nm). The chemical states were analyzed using X-ray photoelectron spectroscopy (XPS) with monochromatic AlKα excitation under vacuum higher than 1×10^{-7} Pa. In addition, Fourier transform-Infrared Radiation (FT-IR) measurement was performed on BRUKER-EQUINOX-55 IR spectrophotometer. All electrochemical measurements were carried out by using a CHI 660E instrument.

1.4 Electrochemical Measurements

The electrochemical measurements were carried out with CHI660e working station in 3.0 M KOH solution at room temperature. Galvanostatic charge-discharge (GCD), Cyclic voltammetry (CV) and electrochemical impedance spectroscopy (EIS) methods were used to investigate the capacitive properties of the Ni-MOF, NiCo-MOF and Co-MOF electrode. The EIS measurements were conducted in the frequency range of 100 kHz to 0.01 Hz at the open-circuit voltage.

For the three-electrode cell, the working electrode was made by mixing the active materials MOF, acetylene black, and polytetrafluoroethylene at a weight ratio of 80 : 15 : 5.

The slurry was coated on a piece of foamed nickel foam (≈ 1 cm^2), which was then pressed into a thin foil at a pressure of 10 MPa. The typical mass loading of the electrode material was 1.0 mg. A platinum electrode and an Hg/HgO electrode served as the counter and reference electrode, respectively.

When assembling an aqueous device, MOF materials was employed as positive electrode while negative electrode was activated carbon. The positive and negative electrodes were made by mixing as-prepared MOF/activated carbon, acetylene black and polytetrauoroethylene at a weight ratio of 80: 15: 5. The slurry was coated on a piece of foamed nickel foam (≈1 cm^2), which was then pressed into a thin foil at a pressure of 10 MPa. The mass ratio of the positive/negative electrode active material was 1: 4, and electrochemical performance was measured in an aqueous device at room temperature.

2 Calculations

The specific capacitance of the electrode material can be calculated from the charge-discharge curves according to the equation:

$$C\ (Fg^{-1}) = Q / (m \times \Delta V) = \int Idt / (m \times \Delta V) = I \times t_{discharge} / (m \times \Delta V) \quad (1)$$

$$C\ (mAh\ g^{-1}) = I \times t_{discharge} / 3600 \times 1000 \quad (2)$$

Where m is the weight of the electrode materials, I is the discharge current, $t_{discharge}$ is discharge time, ΔV is the potential drop during discharge (excluding the *IR* drop).

The energy density (E) and s power density (P) are calculated using equations:

$$E = 1/2 \times C\ (F\ g^{-1}) \times (\Delta V)^2 / 3.6 \quad (3)$$

$$P = 3600 \times E / \Delta t \quad (4)$$

Where E is energy density in Wh kg^{-1}, P is power density in W kg^{-1}, $C(F\ g^{-1})$ is specific capacitance in F g^{-1}, Δt is the discharging time in s, ΔV is the potential window in V.

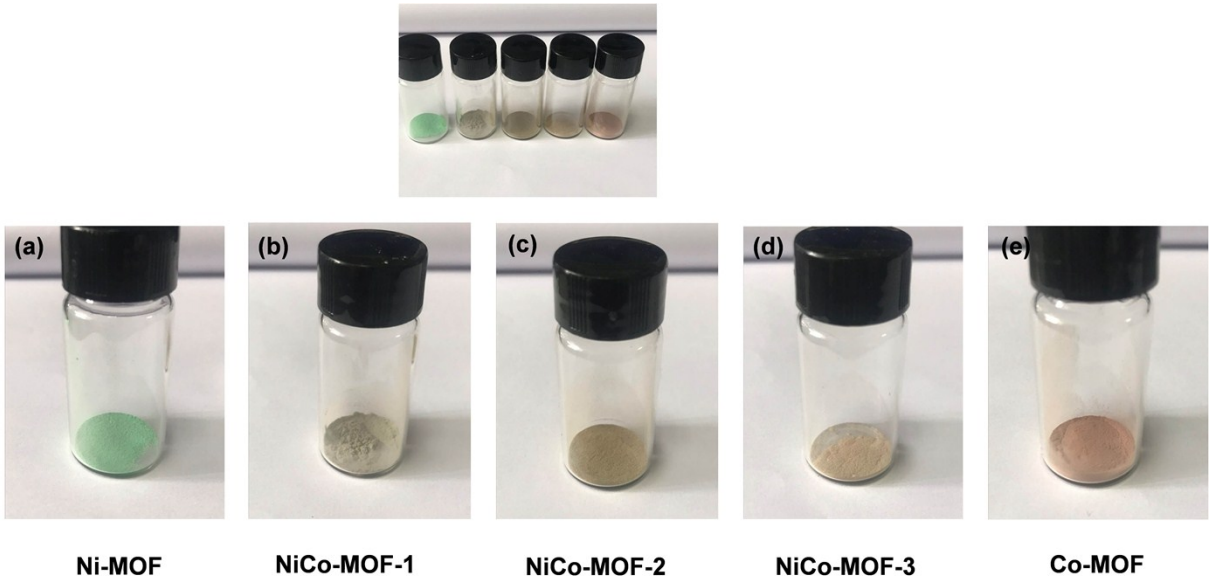

Figure S1. (a-e) Digital Photos of five MOF samples. (sample with a Ni/Co molar ratio of 2:1 is denoted as NiCo-MOF-1, samples with Ni/Co molar ratio of 1:1 and 1:2 are corresponding to NiCo-MOF-2, NiCo-MOF-3, respectively).

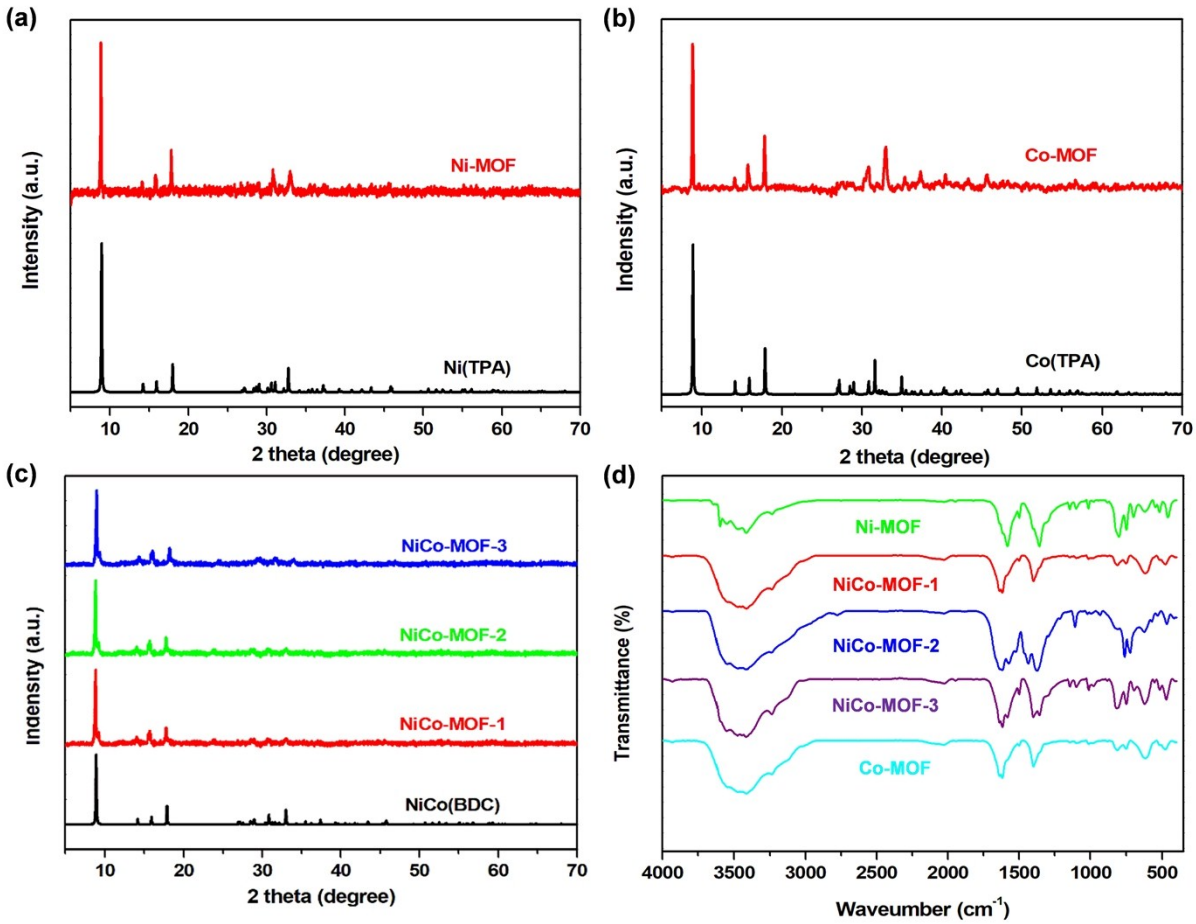

Figure S2. XRD pattern of (a) Ni-MOF, b) Co-MOF, c) NiCo-MOF; (d) FT-IR spectra of the Ni-MOF, Co-MOF, NiCo-MOF-1, NiCo-MOF-2, NiCo-MOF-3.

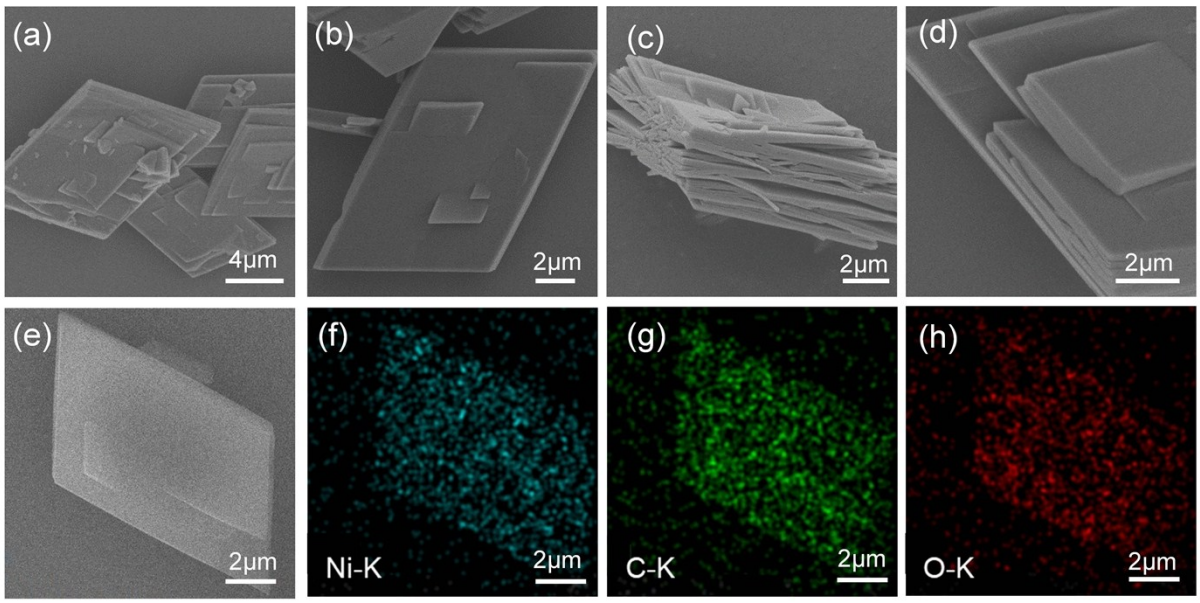

Figure S3. (a-d) SEM images of Ni-MOF; (e-f) The EDS mapping images of Ni-MOF.

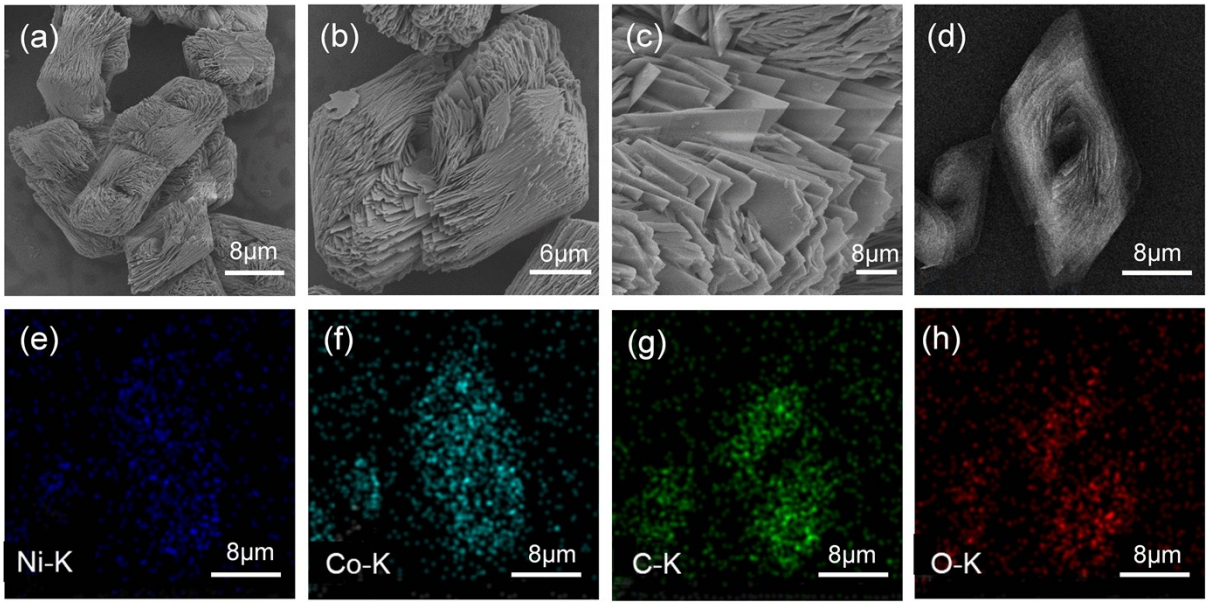

Figure S4. (a-c) SEM images of NiCo-MOF-2; (d-h) The EDS mapping images of NiCo-MOF-2.

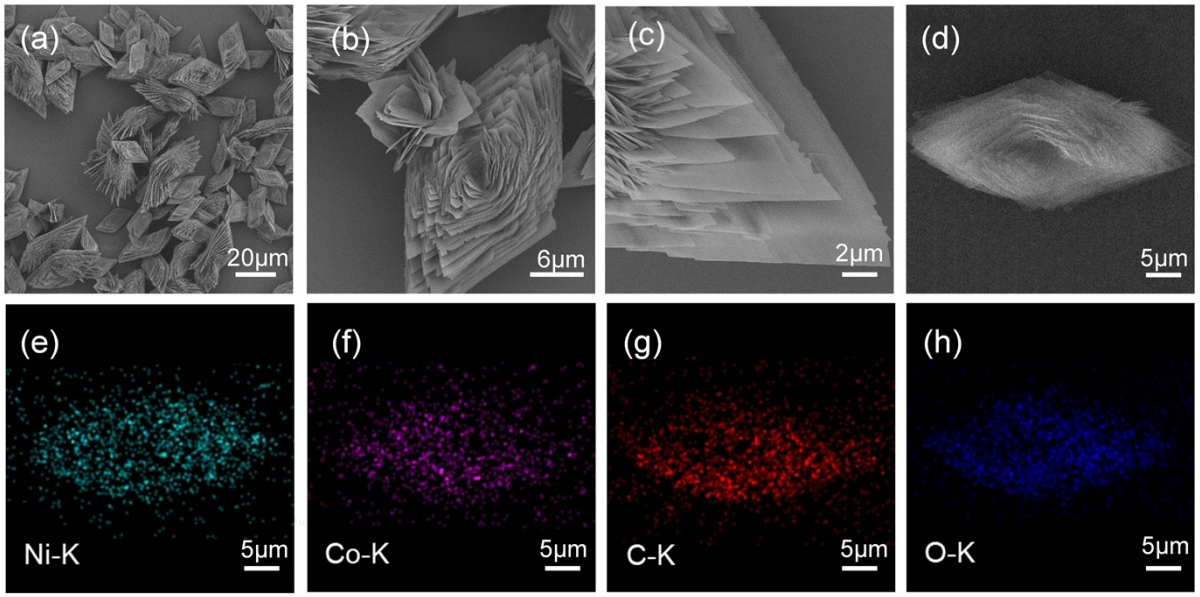

Figure S5. (a-c) SEM images of NiCo-MOF-3; (d-h) The EDS mapping images of NiCo-MOF-3.

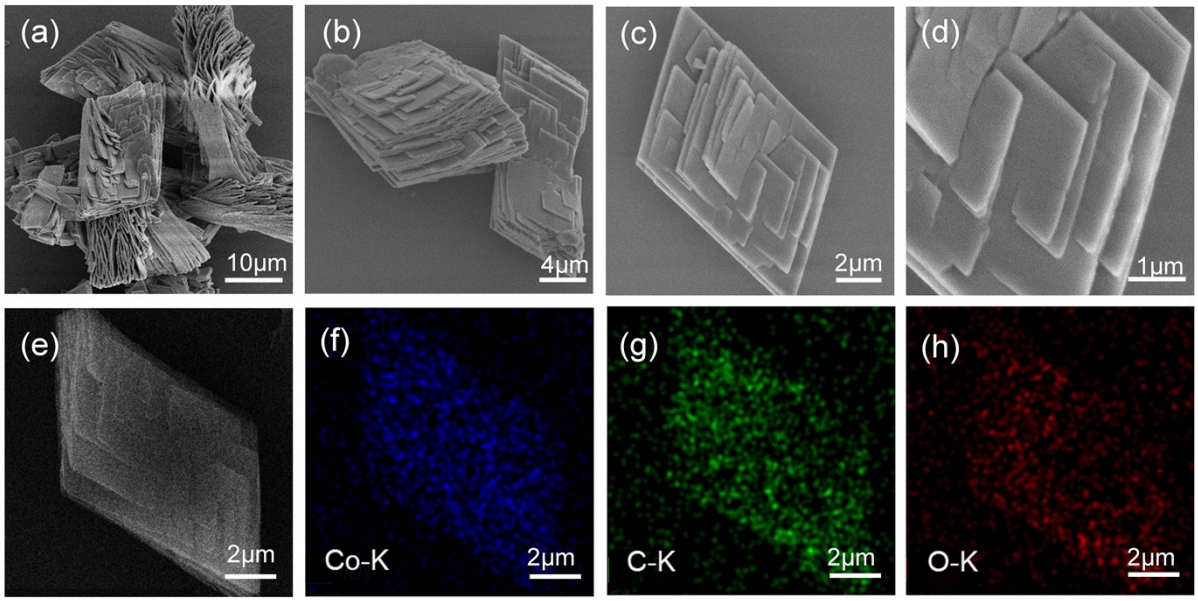

Figure S6. (a-d) SEM images of Co-MOF; (e-f) The EDS mapping images of Co-MOF.

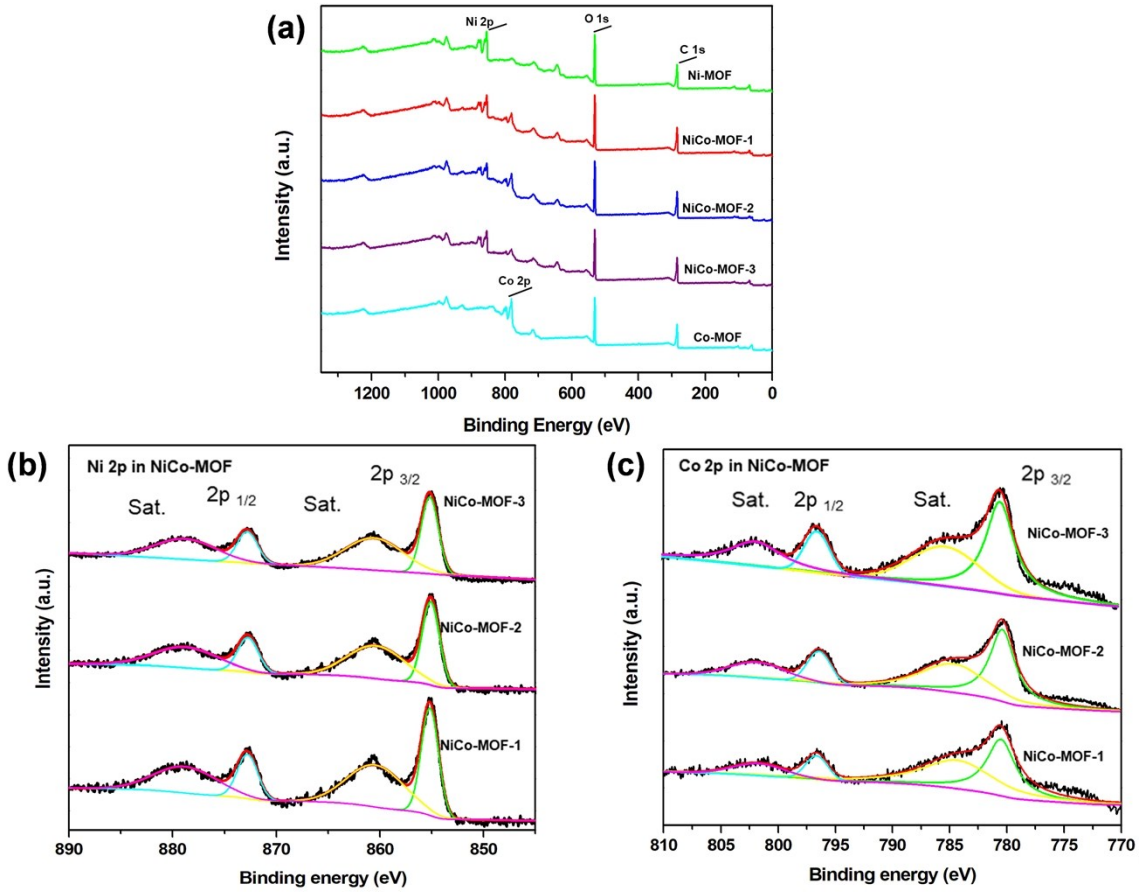

Figure S7. XPS spectra: (a) survey scan of Ni-MOF, NiCo-MOF-1, NiCo-MOF-2, NiCo-MOF-3, Co-MOF; (b) Ni 2p scan of and (c) Co 2p scan of Ni/Co-MOF.

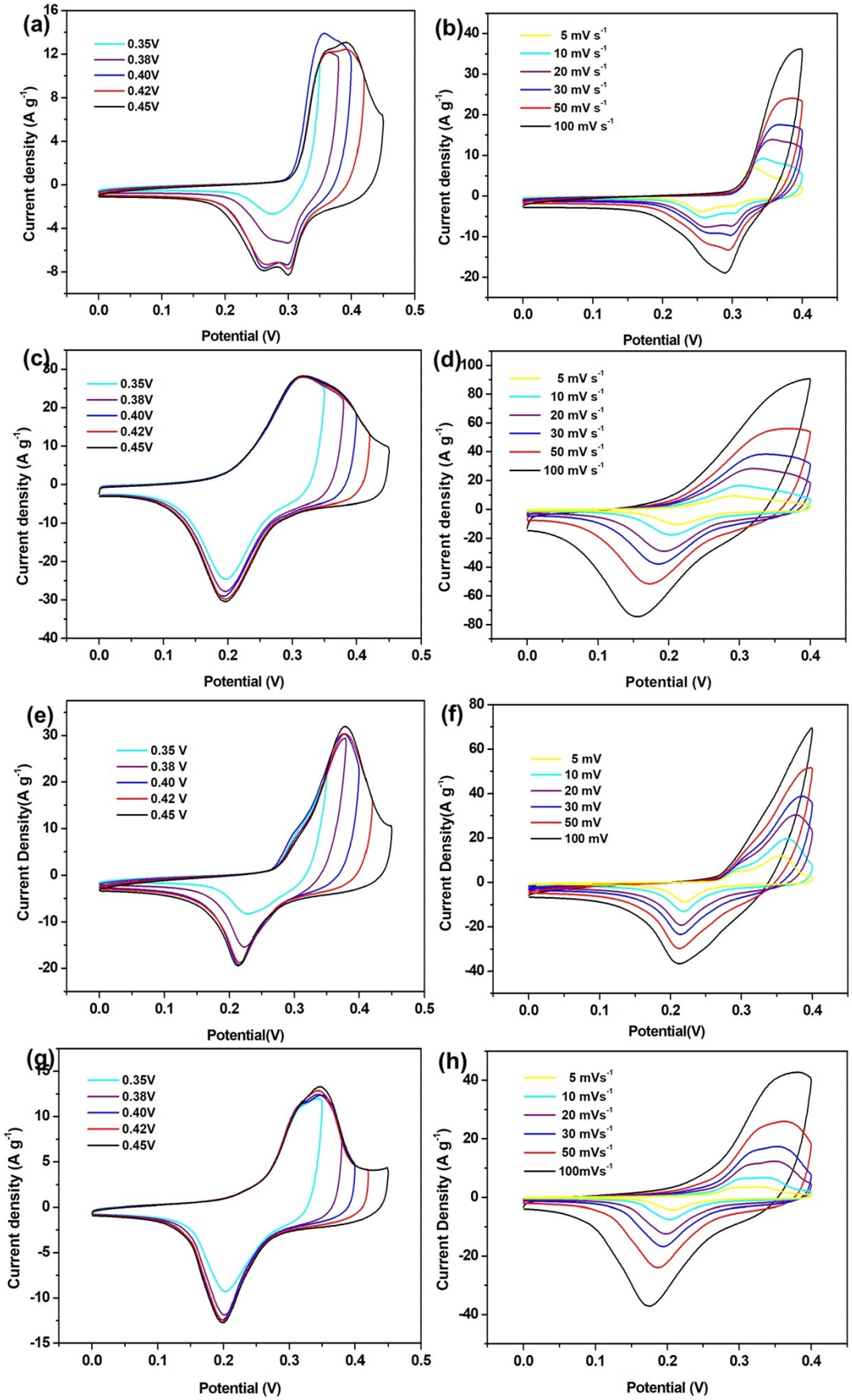

Figure S8. In a three three-electrode system (Hg/HgO as reference electrode), CV curves of (a,b) Ni-MOF, (c-d) NiCo-MOF-2, (e,f) NiCo-MOF-3 and (g,h) Co-MOF.

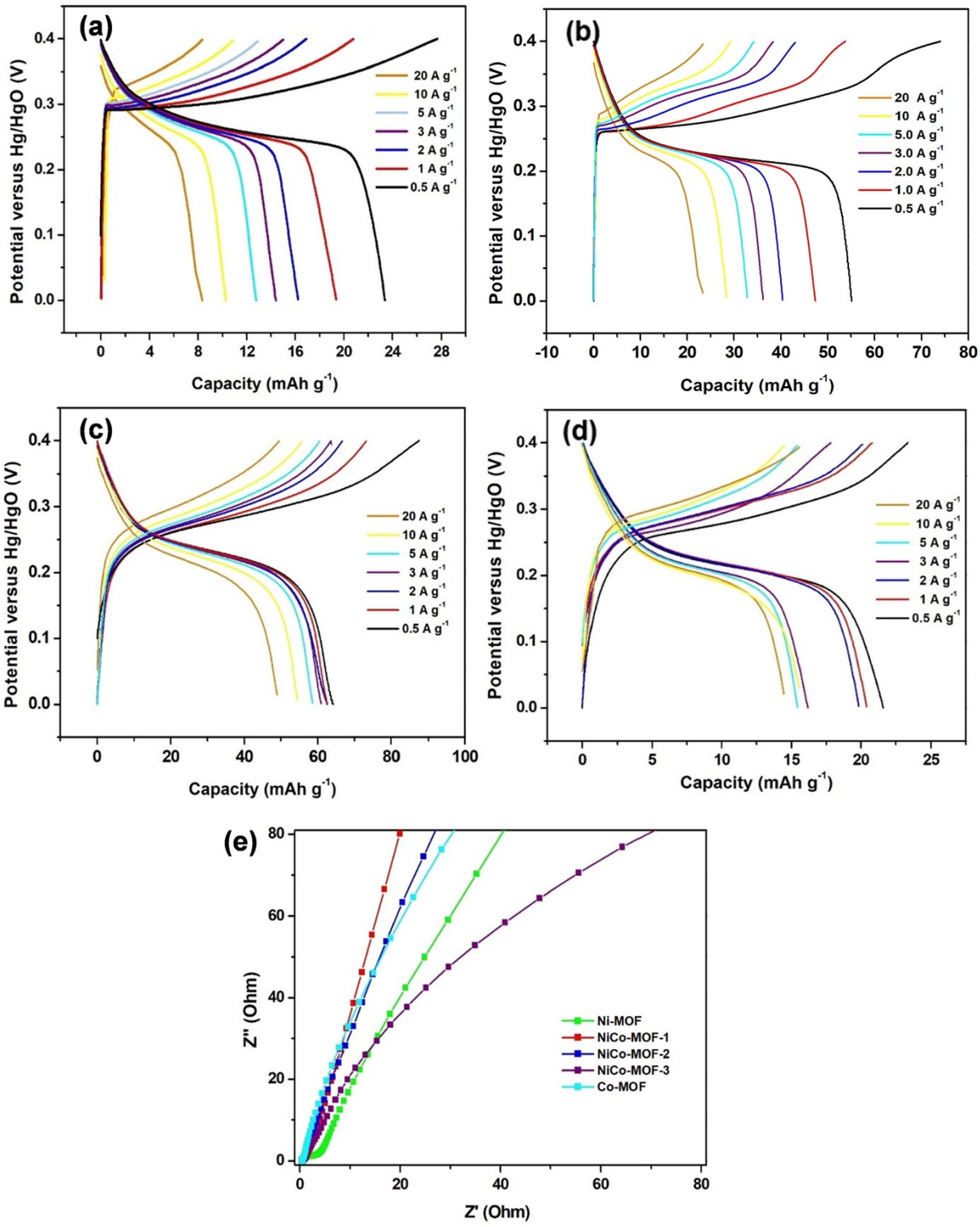

Figure S9. Charge–discharge curves at various current densities of (a) Ni-MOF, (b) NiCo-MOF-2, (c) NiCo-MOF-3 and (d) Co-MOF; (e) EIS spectra of of the five MOF samples.

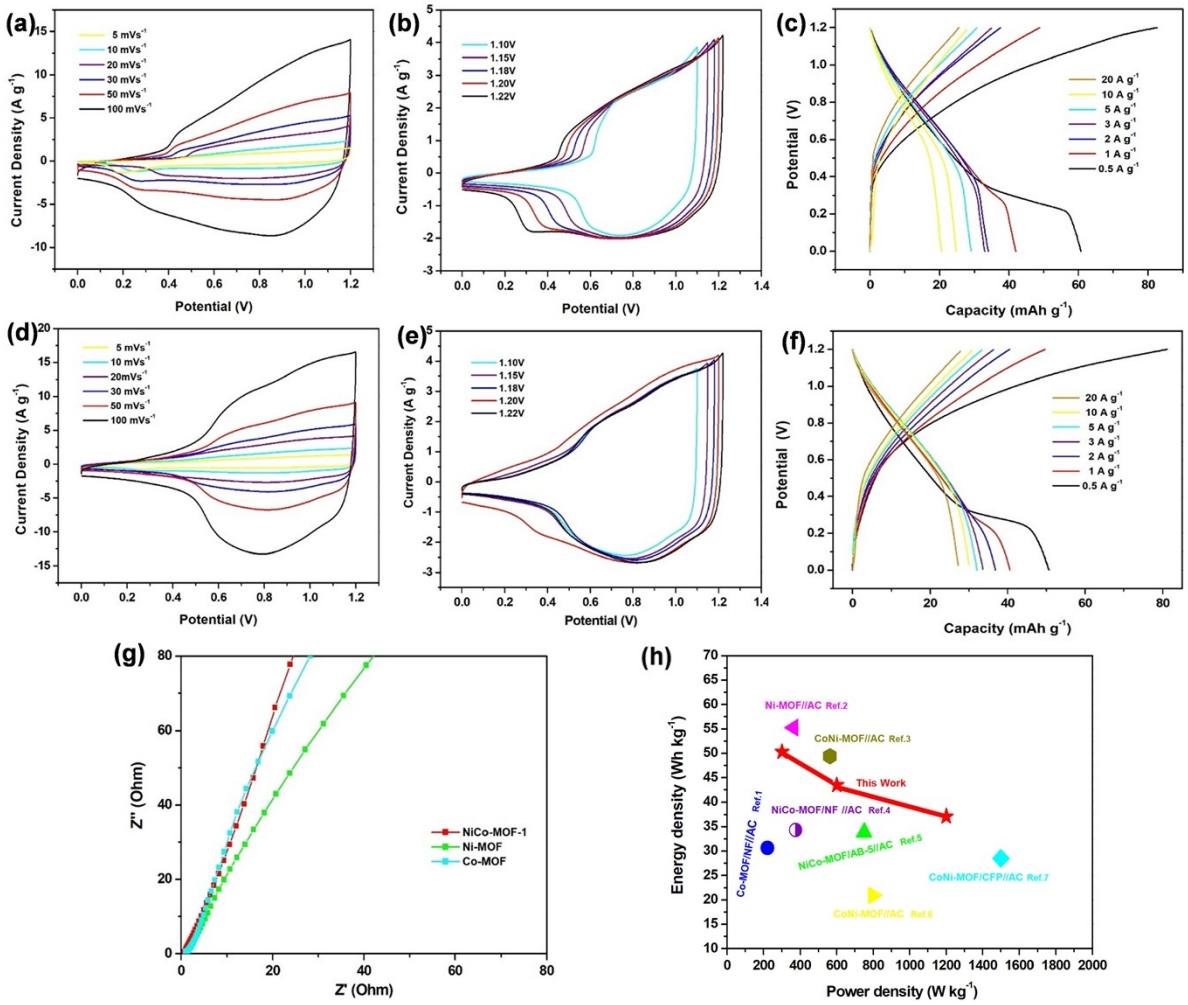

Figure S10. In the aqueous device, (a,b) CV curves and (c) charge–discharge curves of Ni-MOF; (d,e) CV curves and (f) charge–discharge curves of Co-MOF; (g) EIS spectra of the Ni-MOF, NiCo-MOF-1and Co-MOF samples; (h) Ragone plots of the as-prepared aqueous device. The values reported for other aqueous devices are added for comparison.[1-7]

Samples	Electrolyte	Current density [A g^{-1}]	Capacitance [F g^{-1}]/[mA g^{-1}]	Capacitance retention	Ref.
Dandelion-like NiCo-MOF	2M KOH	1	758(101.06)	75%(5000)	1
NiCo-MOF	2M KOH	2	1044(130.50)	94%(5000)	2
NiCo-MOF nanosheet	2M KOH	1	1202(166.95)	89%(5000)	3
NiCo-MOF/nickel foam	6M KOH	1	2230(278.75)	69%(6000)	6
Ni/Co-MOF	3M KOH	1	1067(118.55)	68%(2500)	8
Binary Co–Ni-based MOF	2M KOH	1	979(122.36)	78%(3000)	9
NiCo-MOF nanosheet	2M KOH	1	1140(158.33)	76%(3000)	10
NiCo-MOF	2M KOH	1	990(110.00)	56%(3000)	11
NiCo-MOF	3M KOH	1	1049(116.56)	97%(5000)	12
Hydrangea-like NiCo-MOF	2M KOH	0.5	1057(132.13)	43%(1000)	13
NiCo-MOF	3M KOH	1	902(100.18)	81%(3000)	**This work**

Table S1. A comparison between the superior performance of the Ni-MOF-1 and other recently published NiCo-MOF materials.

References

1 S. Gao, Y. Sui, F. Wei, J. Qi, Q. Meng, Y. Ren and Y. He, *J. Colloid Interface Sci.*, 2018, **531**, 83–90.

2 T. Deng, Y. Lu, W. Zhang, M. Sui, X. Shi, D. Wang and W. Zheng, *Adv. Energy Mater.*, 2018, **8**, 1702294.

3 Y. Wang, Y. Liu, H. Wang, W. Liu, Y. Li, J. Zhang, H. Hou and J. Yang, *ACS Appl. Energy Mater.*, 2019, **2**, 2063–2071.

4 X. Ou, Y. Wang, S. Lei, W. Zhou, S. Sun, Q. Fu, Y. Xiao and B. Cheng, *Dalt. Trans.*, 2018, **47**, 14958–14967.

5 Y. Li, Y. Xu, Y. Liu and H. Pang, *Small*, 2019, **15**, 1902463.

6 J. Wang, Q. Zhong, Y. Zeng, D. Cheng, Y. Xiong and Y. Bu, *J. Colloid Interface Sci.*, 2019, **555**, 42–52.

7 Y. Liu, Y. Wang, H. Wang, P. Zhao, H. Hou and L. Guo, *Appl. Surf. Sci.*, 2019, **492**, 455–463.

8 S. Zhao, L. Zeng, G. Cheng, L. Yu and H. Zeng, *Chinese Chem. Lett.*, 2019, **30**, 605–609.

9 C. Xu, Y. Feng, Z. Mao, Y. Zhou, L. Liu, W. Cheng, J. Wang, H. Shi and X. Liu, *J. Mater. Sci. Mater. Electron.*, 2019, **30**, 19477–19486.

10 X. Zhang, J. Wang, X. Ji, Y. Sui, F. Wei, J. Qi, Q. Meng, Y. Ren and Y. He, *J. Alloys Compd.*, 2020, **825**, 154069.

11 X. Wang, Q. Li, N. Yang, Y. Yang, F. He, J. Chu, M. Gong, B. Wu, R. Zhang and S. Xiong, *J. Solid State Chem.*, 2019, **270**, 370–378.

12 H. Gholipour-Ranjbar, M. Soleimani and H. R. Naderi, *New J. Chem.*, 2016, **40**, 9187–9193.

13 Q. Li, X. Wang, N. Yang, F. He, Y. Yang, B. Wu, J. Chu, A. Zhou and S. Xiong, *Zeitschrift für Anorg. und Allg. Chemie*, 2019, **645**, 1022–1030.